View metadata, citation and similar papers at core.ac.uk

brought to you by CORE

provided by Biblioteca Digital da Produção Intelectual da Universidade de São Paulo (BDPI/USP)

Universidade de São Paulo

Biblioteca Digital da Produção Intelectual - BDPI

Departamento de Engenharia de Materiais - EEL/LOM

Artigos e Materiais de Revistas Científicas - EEL/LOM

2012-06

Boron site preference in ternary Ta and Nb boron suicides

JOURNAL OF SOLID STATE CHEMISTRY, SAN DIEGO, v. 190, n. 11, pp. 1-7, JUN, 2012
http://www.producao.usp.br/handle/BDPI/34519

Downloaded from: Biblioteca Digital da Produção Intelectual - BDPI, Universidade de São Paulo

Journal of Solid State Chemistry 190 (2012) 1–7

Contents lists available at SciVerse ScienceDirect

Journal of Solid State Chemistry

journal homepage: www.elsevier.com/locate/jssc

Boron site preference in ternary Ta and Nb boron silicides

Atta U. Khan [a], Carlos A. Nunes [b], Gilberto C. Coelho [b,c], Paulo A. Suzuki [b], Andriy Grytsiv [a], Francoise Bourreé [d], Gerald Giester [e], Peter F. Rogl [a,*]

[a] Institute of Physical Chemistry, University of Vienna, Währingerstrasse 42, A-1090 Wien, Austria
[b] Escola de Engenharia de Lorena (EEL), Universidade de São Paulo (USP), Polo Urbo-Industrial Gleba AI-6, Caixa Postal 116, 12602-810 Lorena, SP, Brazil
[c] Mestrado Profissional em Materiais, Centro Universitário de Volta Redonda, Av. Paulo Erlei Alves Abrantes 1325, 27240-560 Volta Redonda-RJ, Brazil
[d] Laboratoire L. Brillouin, CEA/Saclay, F-91191 Gif sur Yvette, France
[e] Institute of Mineralogy and Crystallography, University of Vienna, Althanstrasse14, A-1090 Wien, Austria

ARTICLE INFO

Article history:
Received 18 October 2011
Received in revised form
25 January 2012
Accepted 29 January 2012
Available online 4 February 2012

Keywords:
A. Metal boron silicides
B. Crystal structure
C. Microstructure
D. X-ray diffraction.

ABSTRACT

X-ray single crystal (XSC) and neutron powder diffraction data (NPD) were used to elucidate boron site preference for five ternary phases. $Ta_3Si_{1-x}B_x$ ($x=0.112(4)$) crystallizes with the Ti_3P-type (space group $P4_2/n$) with B-atoms sharing the 8*g* site with Si atoms. Ta_5Si_{3-x} ($x=0.03(1)$; Cr_5B_3- type) crystallizes with space group $I4/mcm$, exhibiting a small amount of vacancies on the 4*a* site. Both, $Ta_5(Si_{1-x}B_x)_3$, $x=0.568(3)$, and $Nb_5(Si_{1-x}B_x)_3$, $x=0.59(2)$, are part of solid solutions of M_5Si_3 with Cr_5B_3-type into the ternary M–Si–B systems (M=Nb or Ta) with B replacing Si on the 8*h* site. The $D8_8$-phase in the Nb–Si–B system crystallizes with the Ti_5Ga_4-type revealing the formula $Nb_5Si_3B_{1-x}$ ($x=0.292(3)$) with B partially filling the voids in the 2*b* site of the Mn_5Si_3 parent type.

© 2012 Elsevier Inc. All rights reserved.

1. Introduction

With good properties at high temperatures, boron-silicides of refractory transition metals (TM) are promising materials for high temperature applications [1], particularly the solid solution phases with stoichiometry $(TM1,TM2)_5(Si,B)_3$ exhibit good oxidation resistance, high yield stress and compressive strength and good creep-resistance [2–5]. In some TM–Si–B systems the $(TM)_5(Si,B)_3$ phases are found in equilibrium with the parent metal matrix in the form of a disperse eutectic structure (in-situ metal-matrix composite), providing a good base for the development of high-temperature structural materials. In contrast to the Ta–Si–B system, extended efforts focused on phase equilibria in the Nb–Si–B system [6–10], for which a critical assessment was presented by Korniyenko et al. [11]. A recent thermodynamic modeling of the Nb-rich part of Nb–Si–B system includes a liquidus projection [12]. The ternary compounds or solution phases involved crystallize essentially in three structure types: Cr_5B_3, W_5Si_3 and Mn_5Si_3-type, which all three are characteristic for binary transition metal silicides TM_5Si_3. Depending on the stabilizing influence of boron atoms either in substitutional solutions $(TM)_5(Si,B)_3$ or as interstitials, we observe ternary compounds or extended solid solutions, which, depending on the temperature, may connect with the corresponding binary structure modification. Modern materials design relies on thermodynamic description of equilibrium as well as non-equilibrium phase relations and solidification paths in multi-component systems. A trustable description is based on reliable thermodynamic stabilities of compounds and solution phases either from calorimetric data or from density functional theory (DFT) calculations. It has been demonstrated in the past that fast DFT calculations can provide ground state energies of compounds and solutions with higher precision than slow calorimetric experiments that suffer from incomplete reactions and/or sample contamination. DFT calculations, however, need precise information on crystal structure data, particularly on crystal symmetry and atom site distribution.

Although compounds and solution phases in both systems {Nb,Ta}–Si–B have been unambiguously identified in the past there is a lack of high precision crystal structure investigations and particularly on the site preference of boron. Due to the low atomic number of B, it is difficult to precisely locate this element besides much heavier atoms such as niobium and particularly tantalum via powder X-ray or synchrotron diffraction techniques. As a task of current investigation, Neutron Powder Diffraction (NPD) has been employed to shed more light on crystal symmetry and particularly on the B/Si site occupation and boron/vacancy distribution for the two compounds of the Nb–Si–B system with Cr_5B_3 and Mn_5Si_3-type, respectively. The study was complemented by a search for novel compounds in the Ta–Si–B system,

* Corresponding author. Fax: +43 1 4277 9524.
E-mail address: peter.franz.rogl@univie.ac.at (P.F. Rogl).

0022-4596/$ - see front matter © 2012 Elsevier Inc. All rights reserved.
doi:10.1016/j.jssc.2012.01.060

where two single crystals were extracted from alloys to study via X-ray single crystal (XSC) analyses B/Si site occupation and vacancies in the crystal structures of $Ta_3(Si_{1-x}B_x)$ in comparison with binary Ta_5Si_{3-x}. By chance also a single crystal of $Ta_3Si_{1-x}B_x$ was found in a ternary alloy, which enabled us to check on the B-incorporation in binary Ta_3Si.

2. Experimental details

Alloys were prepared from metal ingots of Ta, Nb and pieces of Si and B (purity 99.998 and 99.5 mass %, respectively, Alfa Johnson Matthey GmbH, D) by repeated arc melting under argon (weight loss less than 0.1%). The reguli were then annealed in a W-mesh heated furnace under Hf-gettered argon at 1800 °C for 6 h in case of the Nb–Si–B alloys and at 1900 °C for 120 h for alloys from the Ta–Si–B system, followed by furnace cooling. Lattice parameters and standard deviations were determined by least squares refinements of room temperature X-ray powder diffraction (XRD) data obtained from a Guinier–Huber image plate employing monochromatic Cu $K_{\alpha 1}$ radiation and Ge as internal standard (a_{Ge}=0.565791 nm). XRD-Rietveld refinements were performed with the FULLPROF program [13] with the use of its internal tables for atom scattering factors. Annealed samples were polished using standard procedures and were examined by scanning electron microscopy (SEM). Quantitative compositions were determined on a CAMEBAX SX-50 electron-beam probe microanalyzer (WDX) with an electron beam current of about 15 nA. Pure elements served as standards to carry out the deconvolution of overlapping peaks and background subtraction. Finally the X-ray intensities were corrected for ZAF effects using the INCA-Energy 300 software package [14]. Overall composition of the samples derived from EPMA area scans agree with the nominal values within 1.0 at%.

Single crystals of $Ta_3Si_{1-x}B_x$ and $Ta_5(Si_{1-x}B_x)_3$ were isolated via mechanical fragmentation of a specimen with nominal composition $Ta_{65.0}Si_{20.0}B_{15.0}$, which was annealed at 1900 °C for 120 h, whereas the single crystal for Ta_5Si_3 was selected from an as cast sample with nominal composition Ta_5Si_3. All crystals were inspected on an AXS-GADDS texture goniometer for quality and crystal symmetry prior to X-ray single crystal (XSC) intensity data collection on a four-circle Nonius Kappa diffractometer (CCD area detector and graphite monochromated Mo K_α radiation, λ=0.071069 nm). Orientation matrix and unit cell parameters were derived using the program DENZO [15]. No individual absorption correction was necessary because of the rather regular crystal shape and small dimensions of the investigated specimens. The structures were solved by direct methods and refined with the SHELXS-97 and SHELXL-97 programs [16], respectively.

Two samples with nominal compositions $Nb_{57.0}Si_{10.0}B_{33.0}$ and $Nb_{62.0}Si_{16.0}B_{22.0}$ were prepared from ^{11}B (chemical purity 99.8% with 96% ^{11}B isotopic enrichment) for neutron powder diffraction (NPD) by annealing at 1800 °C for 6 h and were powdered to a grain size below 40 μm in order to reduce preferential orientation effects. Neutron powder diffraction at room temperature was performed at the ORPHEE 14 MW-reactor (CEA-Saclay) using the 3T2 double-axis multi-detector neutron powder diffractometer at a resolution of $\Delta d/d \geq 4\times10^{-3}$ ($\lambda_{neutron}$=0.12251 nm) [17]. Further details concerning the experiments are summarized in Table 1(a) and (b). Precise atom parameters, occupation numbers, individual isotropic thermal factors and profile parameters were derived from a least squares full matrix Rietveld refinement routine (FULLPROF program [13] with internal neutron scattering lengths). The various reliability factors calculated are defined in Table 1(a) and (b). Using the DIDODATA program [19] we derived the Voronoi coordination polyhedra for all atom sites in the compounds investigated.

3. Results and discussion

3.1. The crystal structure of $Ta_3(Si_{1-x}B_x)$, x=0.112(4) (Ti_3P-type)

Although the structure of binary Ta_3Si (Ti_3P-type) has already been resolved from X-ray powder diffraction [20], no data on site preference and solubility of B in Ta_3Si have been reported. Therefore, a single crystal was selected from a three-phase sample with nominal composition $Ta_{65.0}Si_{20.0}B_{15.0}$ (at %, annealed at 1900 °C) assuring that the composition determined by EPMA ($Ta_{75.2}Si_{21.3}B_{3.5}$) corresponds to the maximum solubility of B in binary Ta_3Si at this temperature.

Lattice parameters obtained from a single crystal [a=1.0183(5) and c=0.5169(3) nm] were close to those reported in the literature for binary Ta_3Si [a=1.017–1.0193 and c=0.516–0.5183 nm] [20–23] indicating a rather low amount of B in solid solution. Systematic extinctions revealed a primitive unit cell with one possible space group symmetry $P4_2/n$ (No. 86). In total, 4 crystallographic sites (all 8g) were obtained, out of which three were fully occupied by Ta and one was a position (M) randomly shared by a mix of 88.8% of Si and 11.2% of B atoms (Table 1(a) and (b)). The refined composition ($Ta_{75.0}Si_{22.2}B_{2.8}$) is close to the EPMA value ($Ta_{75.2}Si_{21.3}B_{3.5}$). With anisotropic displacement parameters, the structure refinement finally converged to R_{F2}=0.022 with little residual electron density (2.59 and $-2.38\times10^3 e^-/nm^3$). Positional parameters (x, y, z) and interatomic distances obtained in the present study were very close to those obtained for binary Ta_3Si [20–23]. We confirmed the coordination figures for the individual atom sites as hitherto described, however, we found 15 ligands for Ta2 (Fig. 1(a) in contrast to the description in the literature (14 ligands) [24].

3.2. The crystal structure of Ta_5Si_{3-x}, x=0.03(1) (Cr_5B_3-type)

Similar to Ta_3Si, the structure of binary Ta_5Si_3 with Cr_5B_3-type is already known in the literature including a Rietveld refinement of X-ray powder diffraction data [23, 25–28]. In order to provide a set of atom positional parameters of higher precision for Ta_5Si_3, single crystal X-ray intensity CCD data were collected. Lattice parameters obtained from the single crystal [a=0.65246(5) and c=1.18853(3) nm] are close to those hitherto reported for the binary Ta_5Si_3-phase (a=0.6511–0.6519 and c=1.1873–1.1887 nm [23, 25–28]). Systematic extinctions confirmed a body centered unit cell with three possible space group symmetries, $I4/mcm$, $I\text{-}4c2$ and $I4cm$. As structure determination using direct methods in all these space groups revealed practically identical solutions, we describe the structure in the space group with the highest symmetry $I4/mcm$ (No. 140). In total, 4 crystallographic sites were obtained, out of which, Si occupied the 4a and 8h sites whilst sites 4c and 16l were fully occupied by Ta. A small defect was found in the 4a site occupied by Si (see Table 1(a) and (b)). The refined composition ($Ta_{63.1}Si_{36.9}$) was close to the composition ($Ta_{62.6}Si_{37.4}$) obtained from EPMA. With anisotropic displacement parameters, the structure refinement finally converged to R_{F2}=0.033 with small residual electron density (7.32 and $-4.88\times10^3 e^-/nm^3$). Fig. 1(b) shows the coordination polyhedra for Ta_5Si_{3-x}, x=0.03(1). The Voronoi analysis excludes the rather long Ta1–Ta1 bond (0.3575 nm) with a very small Voronoi face area (0.10 compared to the maximum area of 4.05) and thus limits the coordination shell for Ta1 to 15 ligands. This is important to mention, because particularly the Ta1–Ta1 bond needs to be included again in the Ta1 polyhedron, when Si is replaced by B in $Ta_5(Si_{1-x}B_x)_3$ (see Section 3.3) and in isostructural $Nb_5(Si_{1-x}B_x)_3$ (see Section 3.4).

3.3. The crystal structure of $Ta_5(Si_{1-x}B_x)_3$, x=0.568(3) (Cr_5B_3- type)

No details on the site preference of B-atoms within the isotypic solid solution $Ta_5(Si_{1-x}B_x)_3$ have been hitherto reported in the

Table 1a
XSC data for $Ta_3(Si_{1-x}B_x)$, $x=0.112(4)$, Ta_5Si_{3-x}, $x=0.03(1)$ and $Ta_5(Si_{1-x}B_x)_3$, $x=0.568(3)$, standardized with program structure tidy [18] and NPD data for $Nb_5(Si_{1-x}B_x)_3$, $x=0.59(2)$ and $Nb_5Si_3B_{1-x}$, $x=0.292(3)$. Isotropic (B_{iso}) and anisotropic (U^{ij}) displacement parameters are given in 10^2nm^2.

Parameter/compound	**$Ta_3(Si_{1-x}B_x)$, $x=0.112(4)$**	**Ta_5Si_{3-x}, $x=0.03(1)$**	**$Ta_5(Si_{1-x}B_x)_3$, $x=0.568(3)$**	**$Nb_5(Si_{1-x}B_x)_3$, $x=0.59(2)$**	**$Nb_5Si_3B_{1-x}$, $x=0.292(3)$**
Method	XSC	XSC	XSC	NPD	NPD
Structure type	Ti_3P	Cr_5B_3	Cr_5B_3	Cr_5B_3	Ti_5Ga_4
Space group	$P4_2/n$, #86	$I4/mcm$, #140	$I4/mcm$, #140	$I4/mcm$, #140	$P6_3/mcm$, #193
Composition from EPMA	$Ta_{75.2}Si_{21.3}B_{3.5}$	$Ta_{62.6}Si_{37.4}$	$Ta_{62.6}Si_{15.5}B_{21.9}$	$Nb_{62.7}Si_{15.8}B_{21.5}$	$Nb_{56.2}Si_{35.8}B_8$
Composition from refinement	$Ta_{75.0}Si_{22.2}B_{2.8}$	$Ta_{63.1}Si_{36.9}$	$Ta_{62.5}Si_{16.2}B_{21.3}$	$Nb_{62.5}Si_{15.3}B_{22.2}$	$Nb_{57.4}Si_{34.5}B_{8.1}$
Formula from refinement	$Ta_3(Si_{1-x}B_x)$, $x=0.112(4)$	Ta_5Si_{3-x}, $x=0.03(1)$	$Ta_5(Si_{1-x}B_x)_3$, $x=0.568(3)$	$Nb_5(Si_{1-x}B_x)_3$, $x=0.59(2)$	$Nb_5Si_3B_{1-x}$, $x=0.292(3)$
Radiations, λ (nm)	Mo K_α	Mo K_α	Mo K_α	$\lambda_n=0.12251$	$\lambda_n=0.12251$
a (nm)	1.0183(5)	0.65246(5)	0.62603(2)	0.62740(4)	0.75762(1)
c (nm)	0.5169(3)	1.18853(3)	1.16008(4)	1.16443(9)	0.52750(1)
Reflections in refinement	$1144 \geq 4\sigma(F_o)$ of 1185	$302 \geq 4\sigma(F_o)$ of 332	$269 \geq 4\sigma(F_o)$ of 308	250	186
Number of variables	36	17	16	31	28
$R_F=\Sigma\lvert F_o-F_c\rvert/\Sigma F_o$	–	–	–	0.0276	0.0164
$R_B=\Sigma\lvert I_o-I_c\rvert/\Sigma I_o$	–	–	–	0.0503	0.0218
$R_{wP}=[\Sigma w_i\lvert y_{oi}-y_{ci}\rvert^2/\Sigma w_i\lvert y_{oi}\rvert^2]^{1/2}$	–	–	–	0.0869	0.0466
$R_P=\Sigma\lvert y_{oi}-y_{ci}\rvert/\Sigma\lvert y_{oi}\rvert$	–	–	–	0.0657	0.0359
$R_e=[(N-P+C)/\Sigma w_i y_{oi}^2]^{1/2}$	–	–	–	0.0237	0.0217
$R_F^2=\Sigma\lvert F_o^2-F_c^2\rvert/\Sigma F_o^2$	0.022	0.036	0.028	–	–
R_{Int}	0.059	0.049	0.024	–	–
w$R2$	0.048	0.095	0.079	–	–
GOF	1.232	1.133	1.321	–	–
Extinction	0.00253(7)	0.0062(5)	0.0010(2)	–	–
Residual density e$^-$/Å^3; max; min.	2.59; −2.38	7.32; −4.88	3.60; −5.94	–	–
Atom parameters					
Atom site 1	8g (x, y, z)	16l (x, $x+½$, z)	16l (x, $x+½$, z)	16l (x, $x+½$, z)	4d ($^1/_3$, $^2/_3$, 0)
Occ.;	2.00 **Ta1**	1.00 **Ta1**	1.00 **Ta1**	1.00 **Nb1**	1.00 **Nb1**
x, y, z;	0.14704(2), 0.66251(2), 0.22260(5)	0.16438(5), 0.15039(4)	0.16696(5), 0.14102(3)	0.1686(1), 0.1396(1)	–
U_{11}; U_{22}; U_{33};	0.0056(1), 0.0043(1); 0.0048(1)	$U_{11}=U_{22}=0.0039(3)$, $U_{33}=0.0026(4)$	$U_{11}=U_{22}=0.0041(2)$, $U_{33}=0.0015(3)$	–	–
U_{23}; U_{13}; U_{12};	0.00049(7), −0.00031(7), −0.00072(7)	$U_{23}=U_{13}=-0.0003(1)$, $U_{12}=-0.0001(1)$	$U_{23}=U_{13}=-0.0004(1)$, $U_{12}=0.0007(1)$	$B_{iso}=0.21(1)$	$B_{iso}=0.21(1)$
Atom site 2	8g (x, y, z)	4c (0, 0, 0)	4c (0, 0, 0)	4c (0, 0, 0)	6g (x, 0, ¼)
Occ.;	1.00 **Ta2**	1.00 **Ta2**	1.00 **Ta2**	1.00 **Nb2**	1.00 **Nb2**
x, y, z;	0.10542(2), 0.23058(2), 0.52127(5)	–	–	–	0.24651(6)
U_{11}; U_{22}; U_{33};	0.0039(1), 0.0072(1); 0.0047(1)	$U_{11}=U_{22}=0.0029(3)$, $U_{33}=0.0035(4)$	$U_{11}=U_{22}=0.0031(2)$, $U_{33}=0.0007(3)$	–	–
U_{23}; U_{13}; U_{12};	0.00063(7), −0.00012(7), −0.00080(7)	$U_{23}=U_{13}=U_{12}=0$	$U_{23}=U_{13}=U_{12}=0$	$B_{iso}=0.10(3)$	$B_{iso}=0.20(1)$
Atom site 3	8g (x, y, z)	4a (0, 0, ¼)	4a (0, 0, ¼)	4a (0, 0, ¼)	6g (x, 0, ¼)
Occ.;	1.00 **Ta3**	0.92(4) **Si1**	1.00 **Si1**	1.00 **Si1**	1.00 **Si1**
x, y, z;	0.53598(2), 0.06267(2), 0.26293(4)	–	–	–	0.6018(1)
U_{11}; U_{22}; U_{33};	0.0033(1), 0.0041(1); 0.0024(1)	$U_{11}=U_{22}=0.006(2)$, $U_{33}=0.005(3)$	$U_{11}=U_{22}=0.006(1)$, $U_{33}=0.004(2)$	–	–
U_{23}; U_{13}; U_{12};	0.00023(7), 0.00007(7), 0.00007(7)	$U_{23}=U_{13}=U_{12}=0$	$U_{23}=U_{13}=U_{12}=0$	$B_{iso}=0.11(5)$	$B_{iso}=0.32(2)$
Atom site 4	8g (x, y, z)	8h (x, $x+½$, 0)	8h (x, $x+½$, 0)	8h (x, $x+½$, 0)	2b (0, 0, 0)
Occ.;	0.888(4) **Si**+0.112 **B**	1.00 **Si2**	0.854(4) **B**+0.146 **Si**	0.89(3) **B**+0.11 **Si**	0.708(3) **B1**
x, y, z;	0.0457(2), 0.2195(2), 0.0277(4)	0.6298(5)	0.622(1)	0.622(1)	–
U_{11}; U_{22}; U_{33};	0.0039(8), 0.0050(8); 0.0031(7)	$U_{11}=U_{22}=0.003(1)$, $U_{33}=0.007(2)$	$U_{11}=0.003(2)$	–	–
U_{23}; U_{13}; U_{12};	0.0000(6), 0.0000(6), −0.0011(5)	$U_{23}=U_{13}=0$, $U_{12}=-0.001(1)$	–	$B_{iso}=0.05(4)$	$B_{iso}=0.13(2)$

literature. In order to elucidate boron incorporation into the lattice of parent Ta_5Si_3 (see Section 3.2), X-ray structure analysis was employed on a single crystal selected from a multi-phase sample with nominal composition $Ta_{65.0}Si_{20.0}B_{15.0}$ (at %, annealed at 1900 °C). Lattice parameters obtained from the single crystal [$a=0.62603(2)$ and $c=1.16008(4)$ nm] were considerably smaller than those reported in the literature for binary Ta_5Si_3 [$a=0.6511$–0.6519 and $c=1.1873$–1.1887 nm] [23, 25–28] as well as those in Section 3.2, indicating a significant solubility of B. Systematic extinctions confirmed a body centered unit cell with three possible space group symmetries, $I4/mcm$, I-4$c2$ and $I4cm$. As structure determination using direct methods in all these space groups revealed practically identical solutions, we describe the structure in the space group with the highest symmetry $I4/mcm$ (No. 140). In total, 4 crystallographic sites were obtained out of which, 4a was fully occupied by Si, 4c and 16l were fully occupied by Ta, but the 8h site clearly revealed a mixed position occupied by 14.6% of Si and 85.4% of B atoms (Table 1(a) and (b)). At this atom arrangement, the refined composition ($Ta_{62.5}Si_{16.2}B_{21.3}$) was close to the EPMA value ($Ta_{62.6}Si_{15.5}B_{21.9}$). With anisotropic displacement parameters, the structure refinement finally converged to $R_{F2}=0.028$ with little residual electron density

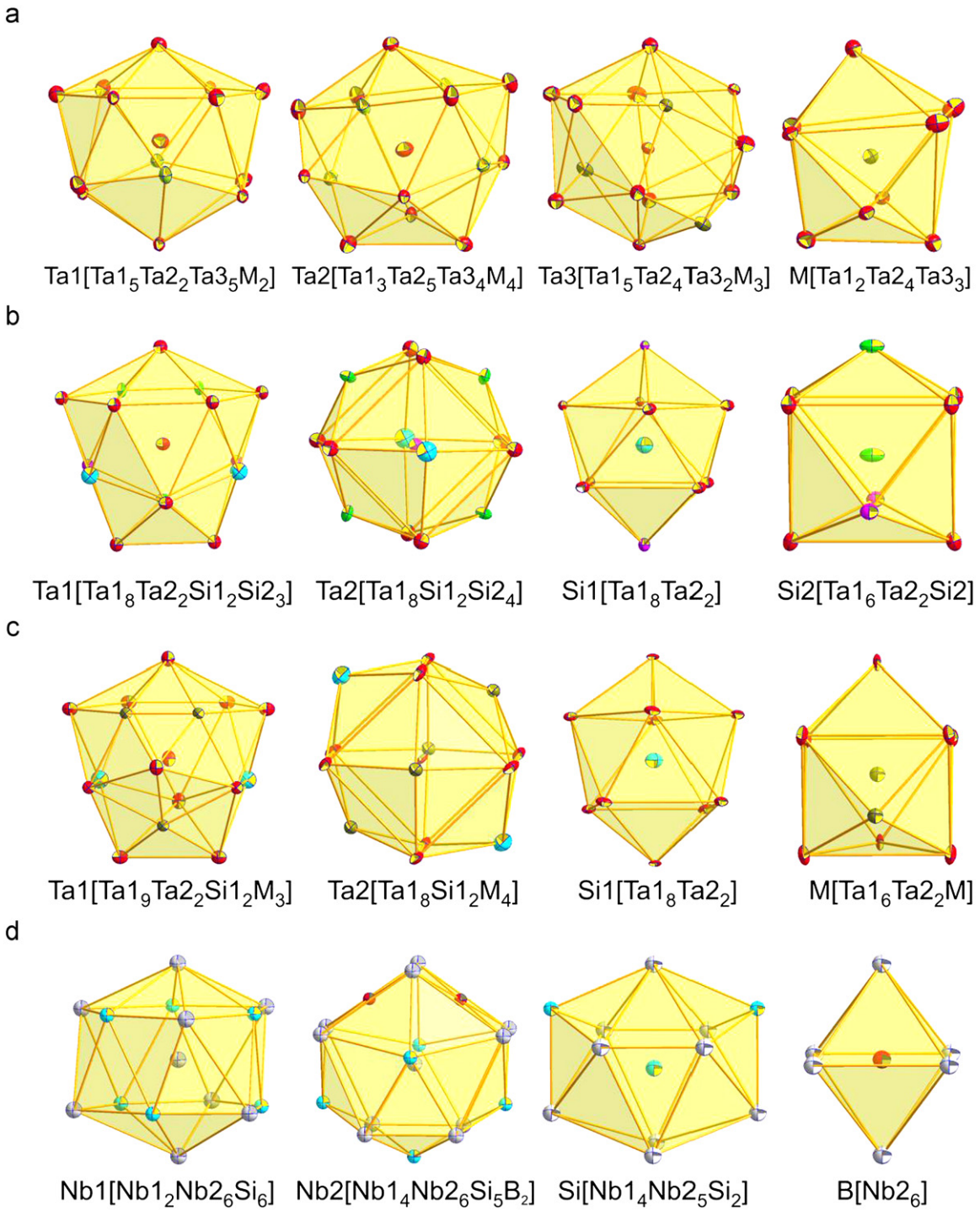

Fig. 1. Coordination polyhedra (a) in $Ta_3(Si_{1-x}B_x)$, $x=0.112(4)$, (b) in Ta_5Si_{3-x}, $x=0.03(1)$, (c) in $Ta_5(Si_{1-x}B_x)_3$, $x=0.568(3)$ and (d) in $Nb_5Si_3B_{1-x}$, $x=0.292(3)$.

(3.60 and $-5.94\times10^3 e^-/nm^3$). Comparing structural parameters for the binary and ternary phases, we can see a significant decrease for the lattice parameters (Table 1(a) and (b)) and for the positional parameters of the 16*l* site (Ta1) as well as of the 8*h* site (M) associated with the Si/B substitution. The shortest bond ($d_{M-M}=0.2163$ nm) is observed between atoms located in the mixed site M (8*h*). Due to the high boron occupation of 85.4% B, the shortest distances between two 8*h* sites (0.2163 nm) are significantly shorter than the corresponding distances in binary Ta_5Si_3 (0.2396 nm). The decrease of the overall atom size in the 8*h* site also influences the positional parameters for the next-nearest Ta1 site (16*l*) and the corresponding distances for the coordination polyhedron of the Ta1 atom (Fig. 1(c). The longest Ta1–Ta1 distance (0.3575 nm), which was excluded in binary Ta_5Si_3 (Section 3.2), becomes considerably shorter (0.3272 nm, Table 1(b)) and again becomes part of the next nearest neighbor polyhedron around Ta1 now having 16 ligands. All other polyhedra keep their shape, but it is noteworthy that several Ta1–(Si/B) distances also shrink significantly (0.2456 nm) as compared to the binary Ta1–Si distances (0.2606 nm), whereas some Ta–Ta distances increase slightly.

It may be noted here, that due to similar atomic size of Nb and Ta, the lattice parameters of $Ta_5(Si_{1-x}B_x)_3$ fit to the compositional dependence of the isotypic Nb-based solid solution, $Nb_5(Si_{1-x}B_x)_3$ [9].

Table 1b
Interatomic distances in nm (standard deviations ≤0.0002) for $Ta_3(Si_{1-x}B_x)$, $x=0.112(4)$, Ta_5Si_{3-x}, $x=0.03(1)$, $Ta_5(Si_{1-x}B_x)_3$, $x=0.568(3)$, $Nb_5(Si_{1-x}B_x)_3$, $x=0.59(2)$ and $Nb_5Si_3B_{1-x}$, $x=0.292(3)$.

$Ta_3(Si_{1-x}B_x)$, $x=0.112(4)$											
Ta1 –	1M	0.2589	CN=15	– 1M	0.2605	Ta3 –	1M	0.2566		– 1Ta1	0.3225
CN=14	– 1M	0.2640		– 1M	0.2625	CN=15	– 1M	0.2663		– 1Ta2	0.3630
	– 1Ta1	0.2752		– 1M	0.2690		– 1M	0.2823		– 1M	0.3805
	– 1Ta3	0.2934		– 1Ta3	0.2879		– 1Ta3	0.2859	M –	1Ta3	0.2566
	– 1Ta3	0.2962		– 1Ta3	0.2901		– 1Ta2	0.2879	CN=9	– 1Ta2	0.2570
	– 1Ta3	0.3063		– 1Ta2	0.2971		– 1Ta2	0.2901		– 1Ta1	0.2589
	– 1Ta2	0.3090		– 1Ta1	0.3090		– 1Ta1	0.2934		– 1Ta2	0.2605
	– 1Ta2	0.3124		– 1Ta3	0.3117		– 1Ta1	0.2962		– 1Ta2	0.2625
	– 1Ta3	0.3189		– 1Ta1	0.3124		– 1Ta1	0.3063		– 1Ta1	0.2640
	– 1Ta3	0.3225		– 2Ta2	0.3163		– 1Ta3	0.3091		– 1Ta3	0.2663
	– 4Ta1	0.3235		– 2Ta2	0.3504		– 1Ta2	0.3117		– 1Ta2	0.2690
Ta2 –	1M	0.2570		– 1Ta3	0.3630		– 1Ta1	0.3189		– 1Ta3	0.2823
Ta_5Si_{3-x}, $x=0.03(1)$											
Ta1 –	1Si2	0.2606		– 1Ta1	0.3034		– 8Ta1	0.3023		– 2Ta1	0.2608
CN=15	– 2Si2	0.2634		– 2Ta1	0.3195	Si1 –	8Ta1	0.2710		– 4Ta1	0.2633
	– 2Si2	0.2710		– 4Ta1	0.3448	CN=10	– 2Ta2	0.2971			
	– 1Ta1	0.2846	Ta2 –	4Si2	0.2558	Si2 –	1Si2	0.2396			
	– 2Ta2	0.3023	CN=14	– 2Si2	0.2971	CN=9	– 2Si2	0.2559			
$Ta_5(Si_{1-x}B_x)_3$, $x=0.568(3)$											
Ta1 –	2M	0.2456		– 1Ta1	0.2956	CN=14	– 8Ta1	0.2849	M –	1M	0.2163
CN=16	– 1M	0.2482		– 1Ta1	0.3272		– 2Si1	0.2900	CN=9	– 4Ta1	0.2456
	– 2Si1	0.2653		– 2Ta1	0.3281	Si1 –	8Ta1	0.2653		– 2Ta1	0.2482
	– 2Ta2	0.2849		– 4Ta1	0.3298	CN=10	– 2Ta2	0.2900		– 2Ta2	0.2486
	– 1Ta1	0.2925	Ta2 –	4M	0.2486						
$Nb_5(Si_{1-x}B_x)_3$, $x=0.59(2)$											
Nb1 –	2M	0.2440		– 1Nb1	0.2992	CN=14	– 8Nb1	0.2843	M –	1M	0.2071
CN=16	– 1M	0.2504		– 1Nb1	0.3252		– 2Si1	0.2911	CN=9	– 4Nb1	0.2440
	– 2Si1	0.2663		– 2Nb1	0.3329	Si1 –	8Nb1	0.2663		– 2Nb1	0.2504
	– 2Nb2	0.2843		– 4Nb1	0.3299	CN=10	– 2Nb2	0.2911		– 2Nb2	0.2514
	– 1Nb1	0.2948	Nb2 –	4M	0.2514						
$Nb_5Si_3B_{1-x}$, $x=0.292(3)$											
Nb1 –	2Nb1	0.2637		– 1Si1	0.2692	Si1 –	2Nb2	0.2637	B1 –	6Nb2	0.2286
CN=14	– 6Si1	0.2668		– 2Si1	0.2877	CN=11	– 4Nb1	0.2668	CN=6		
	– 6Nb2	0.3195		– 4Nb1	0.3195		– 1Nb2	0.2692			
Nb2 –	2B1	0.2286		– 4Nb2	0.3232		– 2Nb2	0.2877			
CN=17	– 2Si1	0.2637		– 2Nb2	0.3235		– 2Si1	0.3056			

3.4. The crystal structure of $Nb_5(Si_{1-x}B_x)_3$, $x=0.59(2)$ (Cr_5B_3-type)

A sample with nominal composition $Nb_{62}Si_{16}B_{22}$ (at %, annealed at 1800 °C) was used for NPD. Lattice parameters [$a=0.62740(4)$, $c=1.16443(9)$ nm] at a B content of 21.5% (after EPMA) fits well with the compositional dependence of parameters for this phase as defined by several authors [6, 8, 9]. Rietveld refinement of the spectrum confirmed the Cr_5B_3-type (Fig. 2, Table 1(a) and (b)) and unambiguously showed that B shares the 8*h* site with Si (0.89B+0.11Si) revealing a composition $Nb_{62.5}Si_{15.3}B_{22.2}$ (at %). This composition is slightly lower than the maximum amount of B in this phase (25%) [9, 10] and it seems that Si will entirely be replaced by B at the limit of the solid solution. It must be noted that no B was found in the 4*a* site (Si1) and thus the boron site preference in this phase is similar to the isotypic solid solution $Ta_5(Si_{1-x}B_x)_3$, ($x=0.568(3)$) in the Ta–Si–B system. Consequently, the influence of Si/B substitution on structural parameters is similar to that observed for the isotypic Ta phase (see Section 3.3). As the coordination polyhedra for this phase are similar to $Ta_5(Si_{0.43}B_{0.57})_3$ (Fig. 1(c) they are not shown here.

3.5. The crystal structure of $Nb_5Si_3B_{1-x}$, $x=0.292(3)$ (Ti_5Ga_4-type)

In order to elucidate via NPD the incorporation of boron atoms in Nb_5Si_3, a sample of nominal composition $Nb_{57}Si_{10}B_{33}$ (at %) was annealed at 1800 °C. Although we were able to index all the diffraction peaks on the basis of a hexagonal lattice that suggested isotypism with the Mn_5Si_3 type, the intensity of some of the peaks was considerably different. Further refinement of this spectrum (Fig. 3) showed that borons do not enter the 6*d* site occupied by Si, but instead occupy the void in the Mn_5Si_3 structure at site 2*b* (0,0,0) at a partial filling level of 71.0% B. Therefore the structure can be considered as a partially filled Mn_5Si_3-type as was first reported by Nowotny et al. [6] ($D8_8$ type). Alternatively the partial filled Mn_5Si_3-type can be considered as a defect Ti_5Ga_4-type [29]. The formula obtained from refinement, $Nb_5Si_3B_{1-x}$ ($x=0.292(3)$), yielded a composition $Nb_{57.4}Si_{34.5}B_{8.1}$, which is in good accord with data from EPMA ($Nb_{56.2}Si_{35.8}B_{8.0}$) (see Table 1(a) and (b)). Furthermore, the refined composition is very close to the point composition shown in the isothermal section by Nunes et al. [10] at 1700 °C and lies inside the homogeneity region presented by Nowotny et al. [6] at 1600 °C. No B content was found for the 6*d* site occupied by Si (Fig. 3) constituting a fully ordered structure except for the B-defects in the 2*b* site. Nb1 atoms have only 14 next nearest neighbors, but interestingly, the Voronoi analysis yielded 17 next nearest neighbors for Nb2 (Fig. 1(d), including B atoms at the center of two square faces in this polyhedron. The coordination polyhedron of B is an octahedron with 6 next nearest neighbors. Although, the calculation prompts 14 nearest neighbors for B, we take only the 6 Nb2 because the distances for the other 8 ligands are rather long (B–B=0.2637 nm and B–Si=0.3292 nm) and cannot be considered as bonding distances. A careful analysis of the neutron diffraction profile excludes the existence of superstructure variants arising from possible ordering among interstitial borons and vacancies in $Nb_5Si_3B_{1-x}$ such as

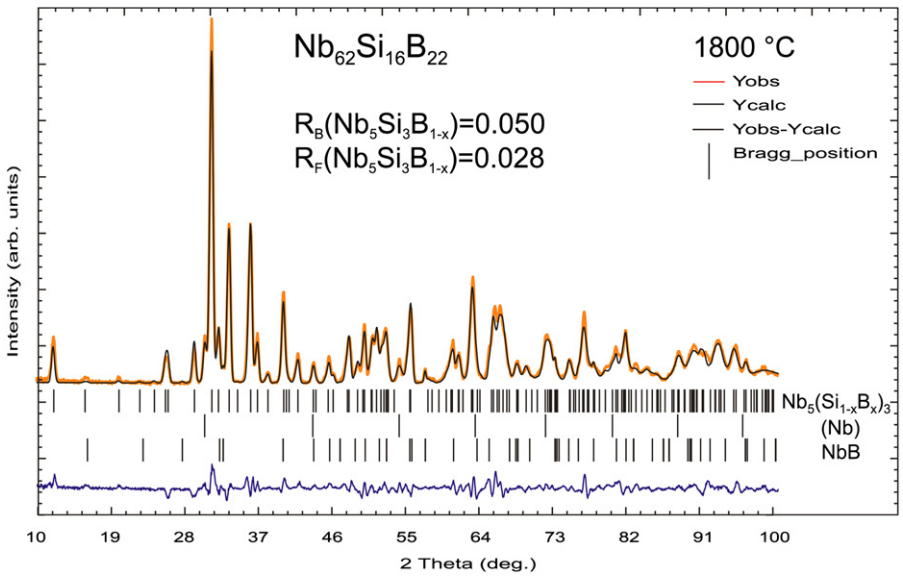

Fig. 2. Rietveld refinement of the NPD spectrum of $Nb_{62}Si_{16}B_{22}$ (nominal composition in at %) revealing the presence of three phases: $Nb_5(Si_{0.41}B_{0.59})_3$, (Nb) and NbB with volume fraction of 91.4, 5.3 and 3.3% obtained from the refinement, respectively.

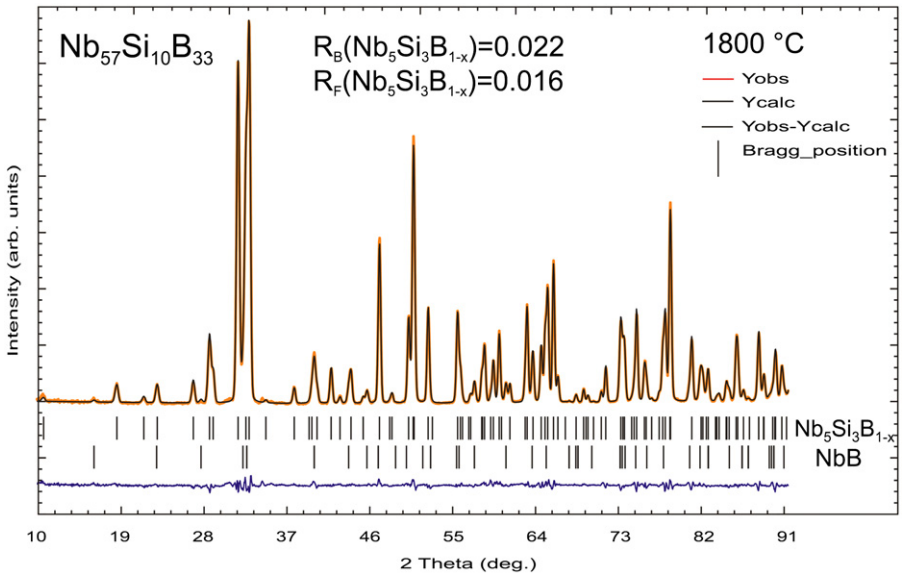

Fig. 3. Rietveld refinement of the NPD spectrum of $Nb_{57}Si_{10}B_{33}$ (nominal composition in at %) showing the presence of two phases: $Nb_5Si_3B_{0.79}$ and NbB with volume fraction of 92.2 and 7.8% obtained from the refinement, respectively.

known for interstitial carbon in partially filled Mn_5Si_3-type phases $RE_5Si_3X_{1-x}$ (RE=rare earth element; X=carbon or boron) [30].

4. Conclusion

The crystal structures of the ternary compounds and solution phases in the metal-rich part of the systems Nb–B–Si and Ta–B–Si have been examined with either X-ray single crystal or neutron powder diffractometry in order to reveal details on the boron site preference and incorporation in binary and ternary structures. $Ta_3(Si_{1-x}B_x)$ (x=0.112(4)) crystallizes with the Ti_3P-type where B and Si atoms randomly share the 8*g* site. Ta_5Si_{3-x} (x=0.03(1)) crystallizes with the Cr_5B_3-type and exhibits a small amount of vacancies on the 4*a* site. For both, $Ta_5(Si_{1-x}B_x)_3$ (x=0.568(3) and $Nb_5(Si_{1-x}B_x)_3$ (x=0.59(2)), the Cr_5B_3-type has been confirmed. The alloys are part of solid solutions $TM_5(Si_{1-x}B_x)_3$ into the ternary TM–Si–B systems where B atoms replace Si on the 8*h* site. In $Nb_5(Si_{1-x}B_x)_3$ (x=0.292(3)) B-atoms partially fill the octahedral voids in the 2*b* site of the parent Mn_5Si_3-type structure (Ti_5Ga_4-type). All these cases demonstrate a strong stabilizing effect of boron incorporation in the Nb,Ta-silicides investigated. The details of atom site occupation will provide the basis (a) for a proper definition of the configurational entropy of the solid solution phases and (b) for a proper definition of the sublattice model in a future thermodynamic modeling of the constitution of the two ternary systems Nb–Si–B and Ta–Si–B. For a most recent DFT study of the Nb-Si-B-T2 phase with Cr_5B_3-type see ref. [31].

Acknowledgments

The research reported herein was supported by the Higher Education Commission of Pakistan (HEC) under the scholarship scheme "PhD in Natural and Basic Sciences from Austria" and the Austrian OEAD. The authors also acknowledge FAPESP (São Paulo,

Brazil), grant 97/06348-4, for financial support. Part of this research was supported by the European Commission under the 6th Framework program through the Key Action: Strengthening the European Research Area, Research Infrastructures; Contract n: RII3-CT-2003-505925.

References

[1] A.J. Thom, E. Summers, M. Akinc, Intermetallics 10 (2002) 555–570.
[2] M.K. Meyer, M.J. Kramer, M. Akinc, Intermetallics 4 (1996) 273–281.
[3] M.K. Meyer, M. Akinc, J. Am. Ceram. Soc. 79 (4) (1996) 938–944.
[4] M.K. Meyer, M. Akinc, J. Am. Ceram. Soc. 79 (10) (1996) 2763–2766.
[5] T.A. Parthasarathy, M.G. Mendiratta, D.M. Dimiduk, Acta Mater. 50 (2002) 1857–1868.
[6] H. Nowotny, F. Benesovsky, E. Rudy, A. Wittman, Monatsh. Chem. 91 (1960) 975–990.
[7] D.M.P. Junior, C.A. Nunes, G.C. Coelho, F. Ferreira, Intermetallics 11 (2003) 251–255.
[8] G. Rodrigues, C.A. Nunes, P.A. Suzuki, G.C. Coelho, Intermetallics 12 (2004) 181–188.
[9] S. Katrych, A. Grytsiv, A. Bondar, P. Rogl, T. Velikanova, M. Bohn, J. Solid State Chem. 177 (2004) 493–497.
[10] C.A. Nunes, D.M.P. Junior, G.C. Coelho, P.A. Suzuki, A.A.A.P. da Silva, R.B. Tomasiello, J. Phase Equilib. Diffus. 32 (2) (2011) 92–96.
[11] K. Korniyenko, P. Rogl, T. Velikanova, MSIT, in: G. Effenberg, S. Ilyenko (Eds.), SpringerMaterials – The Landolt-Börstein Database, Springer-Verlag, Berlin, Heidelberg, . doi:10.1007/978-3-642-02700-0_8.
[12] Z. Sun, Y. Yang, X. Guo, C. Zhang, Y.A. Chang, J. Phase Equlib. Diffus. 32 (2011) 407–411.
[13] T. Roisnel, J. Rodriguez-Carvajal, Mater. Sci. Forum 118 (2001) 378–381.
[14] INCA Energy-300, Oxford Instruments Analytical Ltd., UK 2000.
[15] Nonius Kappa C.C.D., Program Package COLLECT, DENZO, SCALEPACK, SORTAV, Nonius Delft, The Netherlands.
[16] G.M. Sheldrick, SHELXL-97, Program for crystal structure refinement. University of Göttingen, Germany; Windows version by McArdle, Natl Univ. Ireland, Galway; 1997.
[17] M.C. Bellisent-Funel, Neutron News 3 (1) (1992) 7.
[18] L.M. Gelato, E.J. Parthé, Appl. Crystallogr. 20 (1987) 139–143.
[19] E. Koch and W. Fischer, PC versions 9/1997, Z. Kristallogr. 211 (1996), pp. 251–253.
[20] W. Rossteutscher, K. Schubert, Z. Metallkd. 56 (1965) 813–822.
[21] K. Schubert, A. Raman, W. Rossteutscher, Naturwissenschaften 51 (1964) 506–507.
[22] D.K. Deardorff, R.E. Siemens, P.A. Romans, R.A. McCune, J. Less-Common Met. 18 (1969) 11–26.
[23] Y.A. Kocherzhinskii, O.C. Kulik, E.A. Shishkin, Dokl. Akad. Nauk SSSR 261 (1981) 464–465.
[24] P. Villars, K. Cenzual, Pearson's Crystal Data, ASM International, OH, USA, 2010/11. Release.
[25] E. Parthe, H. Nowotny, H. Schmid, Monatsh. Chem. 86 (1955) 385–396.
[26] E. Parthe, B. Lux, H. Nowotny, Monatsh. Chem. 86 (1955) 859–867.
[27] H. Nowotny, C. Brukl, F. Benesovsky, Monatsh. Chem. 92 (1961) 116–127.
[28] H. Nowotny, E. Laube, Planseeber. Pulvermet. 9 (1961) 54–59.
[29] M. Pötzschke, K. Schubert, Z. Metallkd. 53 (1962) 474–488.
[30] G.Y.M. Al-Shahery, I.J. McColm, J. Less-Common Met. 98 (1984) L5.
[31] J.-M. Joubert, C. Colinet, G. Rodrigues, P. A. Suzuki, C.A. Nunes, G.C. Coelho, J.-C. Tedenac; J Solid State Chem., submitted.